Simulation of excited states and the sign problem in the path integral Monte Carlo method

2005 J. Phys. A: Math. Gen. 38 6659

(http://iopscience.iop.org/0305-4470/38/30/003)

INSTITUTE OF PHYSICS PUBLISHING JOURNAL OF PHYSICS A: MATHEMATICAL AND GENERAL

J. Phys. A: Math. Gen. **38** (2005) 6659–6674 doi:10.1088/0305-4470/38/30/003

Simulation of excited states and the sign problem in the path integral Monte Carlo method

Alexander P Lyubartsev

Division of Physical Chemistry, Arrhenius Laboratory, Stockholm University, S 106 91 Stockholm, Sweden

E-mail: sasha@physc.su.se

Received 20 April 2005, in final form 15 June 2005
Published 13 July 2005
Online at stacks.iop.org/JPhysA/38/6659

Abstract

An approach is presented to compute properties of excited states in path integral Monte Carlo simulations of quantum systems. The approach is based on the introduction of several images of the studied system which have the total wavefunction antisymmetric over permutations of these images, and a simulation of the whole system at low enough temperature. The success of the approach relies, however, on the solution of the sign problem for the corresponding system. In the cases when the sign problem may be resolved (as for fermions in one dimension), properties of excited states can be computed with high precision. This was demonstrated by a simulation of excited states of a single particle in one- and two-dimensional harmonic oscillators. An example of the simulation of excited states of several interacting electrons in one dimension is also given.

PACS numbers: 02.70.Ss, 05.30.−d

1. Introduction

The path integral Monte Carlo (PIMC) [1] method is designed for the simulation of systems of interacting quantum particles. It allows us, in principle, to obtain statistically exact equilibrium averages of physical observables in many-body quantum systems at finite temperatures. Despite its clearly fundamental character and seeming simplicity of the computational algorithm, the area of applications of the PIMC technique for simulations of many-body quantum systems is still rather limited. For example, a challenging problem such as accurate computations of the electron structure in atoms and molecules has in fact never been treated by the PIMC approach in a serious manner.

The origin of the difficulties of the PIMC method for the description of electrons is well known: this is the so-called sign problem. The wavefunction, describing N fermions (which electrons are), must change sign (be antisymmetric) upon transposition of any two particles. Hence, the density matrix must also be antisymmetric upon particle transpositions. This results

in alternating signs in the discretized coordinate representation of the density matrix which defines the weight function within the PIMC method. At low temperatures, contributions from positive and negative parts of the weight function almost perfectly cancel each other so that there is no hope of extracting any useful information.

Another principal problem of the PIMC approach is that, while simulating a quantum system at finite temperature, it is generally not possible to extract information on properties of separate excited states. Final results always appear as a mixture of contributions of all eigenstates of the Hamiltonian weighted by the Boltzmann factor. Only the ground state properties can be computed by setting the temperature low enough. In many cases, however, (chemical reactions, spectroscopic problems, etc) knowledge of properties of the first or second excited states is important. The usual quantum-chemical approaches, which work well for the ground states, are much less reliable for the description of excited states.

The two aforementioned problems are in fact closely interconnected. Consider a simple model: two fermionic non-interacting particles without spin (or with the same spin projection) in an external field. If the temperature is low (much less than the energy gap between the energy levels), one particle would occupy the ground state of the system while another would occupy the first excited state. Thus we obtain results (for example, coordinate distribution) which correspond to the sum of the ground and the first excited state. Subtracting the result corresponding to the ground state (obtained for a single-particle simulation in the same potential field), we obtain in this way properties of the first excited state.

Properties of the second, third and upper excited states may be obtained in a similar way by simulating three, four or more non-interacting fermionic particles. Even excited states of several interacting particles may be simulated in a similar fashion, if one considers two 'images' of the system: particles within each image interact with each other, but between different images they do not interact and have only the fermionic antisymmetry of the wavefunction.

Such a method of simulation of excited states faces, however, an evident obstacle: it requires the simulation of a fermionic system at low temperature with the accompanying sign problem. Moreover, the more accurately we would like to compute properties of the excited state, the lower temperature we have to choose and more severe the sign problem will be. Thus, the solution of the problem of excited states simulations relies completely on the solution of the sign problem.

The interconnection of the sign problem and excited state simulations also has another side. There exist approaches aiming at, if not overcoming, relaxing the sign problem: the *restricted path integral* Monte Carlo [2], the *multilevel blocking approach* [3, 4] as well as a number of methods for lattice models [5, 6]. The assumptions within these approaches are not always strictly proved and reproduction of energy levels of known systems by simulating a number of non-interacting fermions may be a good test [7].

The aim of this paper is, using several simple exactly solvable models, to get a deeper insight into the behaviour of PIMC simulations of non-interacting fermion particles, which may help find new strategies to the approach to the solution of the sign problem. Simulation of non-interacting particles allows us to study purely exchange effects, not perturbed by interactions, and how well the exchange effects are reproduced by different simulation techniques. We also explore how far we can go in the solution of the excited state problem for different models. Two in principle exact methods of the simulation of a fermion system, one based on permutation sampling [8] and another on an antisymmetric propagator [9], are considered. The latter approach clearly proved to be superior, allowing us in the one-dimensional case to eliminate the sign problem completely. The two-dimensional harmonic potential (a quantum dot), a three-dimensional Coulombic potential (a hydrogen atom) as well as several interacting electrons in a one-dimensional harmonic trap are also considered.

2. Theory

2.1. PIMC for distinguishable particles

Consider first a system of N distinguishable quantum particles. The standard path integral Monte Carlo approach is based on the following expansion of the density matrix $\hat{\rho}_D$ (known also as the Trotter expansion) [10],

$$\hat{\rho}_D = \exp(-\beta\hat{H}) = \exp\left(-\frac{\beta}{J}\hat{H}\right)\exp\left(-\frac{\beta}{J}\hat{H}\right)\cdots\exp\left(-\frac{\beta}{J}\hat{H}\right) \tag{1}$$

where high-temperature (short-time) density matrices $\exp\left(-\frac{\beta}{J}\hat{H}\right)$ are repeated J times and index D stands for distinguishable particles. In the coordinate representation, expression (1) reads as

$$\hat{\rho}_D\left(x_1^{(1)},\ldots,x_N^{(1)}\middle|x_1^{(J+1)},\ldots,x_N^{(J+1)}\right) = \int\prod_{j=1}^{J}\left(\prod_{i=1}^{N}\mathrm{d}x_i^{(j)}\right)\left\langle x_1^{(j)},\ldots,x_N^{(j)}\right|\exp\left(-\frac{\beta}{J}\hat{H}\right)\left|x_1^{(j+1)},\ldots,x_N^{(j+1)}\right\rangle \tag{2}$$

where the subscript of x refers to the particle number while the superscript refers to the corresponding term in expansion (1) (imaginary time). Each bracket in (2) is a high-temperature density matrix which, at large enough J, may be approximated by

$$\left\langle x_1^{(j)},\ldots,x_N^{(j)}\right|\exp\left(-\frac{\beta}{J}\hat{H}\right)\left|x_1^{(j+1)},\ldots,x_N^{(j+1)}\right\rangle = \left(\frac{J}{2\pi\beta}\right)^{dN/2}\exp\left(-\frac{J}{2\beta}\sum_{i=1}^{N}\left(x_i^{(j)}-x_i^{(j+1)}\right)^2-\frac{\beta}{2J}\left(V\left(\left\{x_i^{(j)}\right\}\right)+V\left(\left\{x_i^{(j+1)}\right\}\right)\right)\right) \tag{3}$$

where d is the dimensionality of the space and $V\left(\left\{x_i^{(j)}\right\}\right)$ is the potential energy of N particles having the same index j. Here and below the reduced units are used in which m (mass), $\hbar$ (the Planck constant) and e (the electron charge) are equal to 1.

The partition function is expressed as *trace* of the density matrix:

$$Z = \mathrm{Tr}(\hat{\rho}_D). \tag{4}$$

After substitution of (2) and (3) into (4) one comes to the well-known path integral representation of the quantum partition function in terms of a configurational integral for N ring 'polymers' with harmonic bonds of rigidity J/β^2 and interacting with potential V/J.

2.2. PIMC for fermions: permutation sampling

The expressions in the previous section are valid for distinguishable particles. If the particles are identical, the density matrix must be antisymmetrized [8, 10] upon particle permutations

$$\rho_A(x_1,x_2,\ldots,x_N|x_1',x_2',\ldots,x_N') = \frac{1}{N!}\sum_P \mathrm{Sign}(P)\rho_D(x_1,x_2,\ldots,x_N|x'_{P(1)},x'_{P(2)},\ldots,x'_{P(N)}) \tag{5}$$

where summation is taken over all permutations on N elements and $\mathrm{Sign}(P)$ is the sign of permutation P. Strictly speaking, variables x must include both coordinates and spin projections. In this paper, only the case of 'spinless' fermions is considered. Though such fermions do not exist, one can consider, for instance, electrons in a state when all the spins have the same projection (polarized electrons). Also, for the problem of excited state

simulations, just spinless fermions are needed. A method accounting for spin in fermionic PIMC simulations was considered, for example, in [11].

The partition function calculated as the *trace* of antisymmetric density matrix ρ_A will then be

$$Z_A = \frac{1}{N!}\sum_P \mathrm{Sign}(P)\left(\frac{J}{2\pi\beta}\right)^{dJN/2}\int\prod_{j=1}^{J}\left(\prod_{i=1}^{N}\mathrm{d}x_i^{(j)}\right) \times \exp\left(-\frac{J}{2\beta}\sum_{j=1}^{J}\left(\sum_{i=1}^{N}\left(x_i^{(j)}-x_i^{(j+1)}\right)^2\right)-\frac{\beta}{J}\sum_{j=1}^{J}\sum_{i=1}^{N}V\left(\left\{x_i^{(j)}\right\}\right)\right) \tag{6}$$

with boundary conditions $x_i^{(1)} = x_{P(i)}^{(J+1)}$. The latter requirement means that the end of the trajectory of the ith particle is linked to the beginning of the trajectory of another, $P(i)$th, particle. This is the standard form of discretized path integrals for fermionic particles which was used in a number of PIMC simulations [2, 11–13]. Schematically, each permutation may be presented as a 'diagram', and the Monte Carlo procedure includes in this case steps moving the beads of trajectories and steps changing permutation (or diagram) in sum (6). Below, this form of PIMC will be referred to as 'permutation sampling' (PS). If the temperature is low, contributions from each diagram become nearly equal and, because of the alternating sign in (6), the total sum becomes exponentially small relative to each term.

2.3. PIMC for fermions: an antisymmetric propagator

In another approach, introduced by Takahashi in 1984 [9], the Trotter expansion acts on an already antisymmetrized density matrix $\hat{\rho}_A$, while antisymmetrization operation (5) is applied to each high-temperature density matrix in the Trotter expansion (2):

$$Z_A = \int\prod_{j=1}^{J}\left(\prod_{i=1}^{N}\mathrm{d}x_i^{(j)}\right)\rho_A^{(j)}\left(x_1^{(j)},\ldots,x_N^{(j)}\middle|x_1^{(j+1)},\ldots,x_N^{(j+1)}\right) \tag{7}$$

Each high-temperature antisymmetric density matrix $\rho_A^{(j)}\left(x_1^{(j)},\ldots,x_N^{(j)}\middle|x_1^{(j+1)},\ldots,x_N^{(j+1)}\right)$ is, in turn, presented as a sum over permutations of high-temperature density matrices for distinguishable particles,

$$\begin{aligned}\rho_A^{(j)}&\left(x_1^{(j)},\ldots,x_N^{(j)}\middle|x_1^{(j+1)},\ldots,x_N^{(j+1)}\right)\\ &= \frac{1}{N!}\left(\frac{J}{2\pi\beta}\right)^{dN/2}\sum_P \mathrm{Sign}(P)\exp\left(-\frac{J}{2\beta}\sum_{i=1}^{N}\left(x_i^{(j)}-x_{P(i)}^{(j+1)}\right)^2\right.\\ &\quad\left.-\frac{\beta}{2J}\left(V\left(\left\{x_i^{(j)}\right\}\right)+V\left(\left\{x_i^{(j+1)}\right\}\right)\right)\right)\\ &= \frac{1}{N!}\left(\frac{J}{2\pi\beta}\right)^{dN/2}\exp\left(-\frac{\beta}{2J}\left(V\left(\left\{x_i^{(j)}\right\}\right)+V\left(\left\{x_i^{(j+1)}\right\}\right)\right)\right)\\ &\quad\times\det\begin{vmatrix}\exp\left(-\frac{J}{2\beta}\left(x_1^{(j)}-x_1^{(j+1)}\right)^2\right) & \ldots & \exp\left(-\frac{J}{2\beta}\left(x_1^{(j)}-x_N^{(j+1)}\right)^2\right)\\ \cdots & \cdots & \cdots\\ \exp\left(-\frac{J}{2\beta}\left(x_N^{(j)}-x_1^{(j+1)}\right)^2\right) & \ldots & \exp\left(-\frac{J}{2\beta}\left(x_N^{(j)}-x_N^{(j+1)}\right)^2\right)\end{vmatrix}\end{aligned} \tag{8}$$

with boundary conditions $x_i^{(1)} = x_i^{(J+1)}$.

Expressions (6) and (7) for the antisymmetric partition function are equivalent due to the cyclic symmetry over index (j) [9], but they imply different implementations of the

MC simulation procedure and thus may show rather different efficiency. In the case of the antisymmetric propagator (7), (8), each trial move of a single bead $x_i^{(j)}$ affects two weights $\rho^{(j-1)}$ and $\rho^{(j)}$ which requires the recalculation of a single potential energy term and two determinants accounting for permutational symmetry. The determinants may be computed by standard algorithms requiring an order of N^3 operations which may be considered as acceptable. After the recalculation of weights, standard Metropolis Monte Carlo rules are applied to decide whether to accept the transition. Also, a more efficient Monte Carlo algorithm may include some collective moves shifting all the beads corresponding to the same index j or even bigger pieces of trajectories.

In this approach, which may be called 'antisymmetric propagator' (AP), partial cancelling of positive and negative weights takes place at each imaginary time moment j. Each of weights, $\rho^{(j)}$, as well as the total weight function, $\prod_j \rho^{(j)}$, may accept both positive and negative values. In this representation, the simulated particles really become identical: due to the presence of determinants, any permutations of beads at some imaginary time moment do not change the total weight function.

A remarkable feature of the AP approach is that for one-dimensional systems, the total weight function in (7) is always positive [9, 14]. Thus, in the one-dimensional case, the sign problem vanishes completely. This fact was also noted for a number of lattice models [15, 16]. It will be shown below that this fact allows us to carry out very accurate calculations of the properties of excited states in the one-dimensional case.

2.4. Calculation of excited states of several interacting particles

The well-known fact concerning Fermi systems is that N non-interacting fermions at low (zero) temperature occupy the N lowest states of a single-particle system in the same external field. This gives us possibility of computing properties of single-particle excited states by successive simulations of one, two and so on fermions. These arguments do not work directly, however, if one would like to compute excited states of several interacting particles. To generalize this approach for the case of several particles, consider the following scheme.

Assume that we have N interacting particles in a d-dimensional space. Let us introduce M imaginary copies of this system. Each image consists of the same number of particles with the same kind of permutation symmetry, interparticle interaction and the external potential as the original system. There is, however, no interaction between particles belonging to different images. Introduce also fermionic symmetry between the images: the total wavefunction (and the total density matrix) changes sign when particles on one image change place with particles of another image.

In fact, each such image of the system of N particles can be considered as a 'superparticle' in $N \cdot d$ dimensions. The superparticles do not interact with each other and have fermionic permutational symmetry. Therefore, at low temperature they fall into M lowest lying states. Using the same logic, one can compute excited states of 'superparticles' by successive simulations of one, two and more of them. The excited states of 'superparticles' would correspond to excited states of n original interacting particles.

It is rather straightforward to generalize the AP approach of Takahashi to simulate such system of M images of N interacting particles by the PIMC method. The Trotter formula is applied to the partition function in the usual manner,

$$Z_M(\beta) = \operatorname{Tr} \exp(-\beta \hat{H}_M) = \operatorname{Tr} \left(\prod_{j=1}^{J} \exp\left(-\frac{\beta}{J} \hat{H}_M \right) \right) \tag{9}$$

where $\hat{H}_M$ is the Hamiltonian describing the system of M images, defined as a sum of (identical) Hamiltonians corresponding to each separate image. In the coordinate representation equation (9) is rewritten as

$$Z_M(\beta) = \int \prod_{j=1}^{J} \left(\prod_{m=1}^{M} \prod_{i=1}^{N} \mathrm{d}x_{i,m}^{(j)} \right) \Re_M^{(j)}\left(x_{1,1}^{(j)}, \ldots, x_{N,M}^{(j)} \middle| x_{1,1}^{(j+1)}, \ldots, x_{N,M}^{(j+1)}\right) \tag{10}$$

where $x_{i,m}^{(j)}$ is the coordinate of the ith particle of the mth image in the jth imaginary time moment and

$$\Re_M^{(j)}\left(x_{1,1}^{(j)}, \ldots, x_{N,M}^{(j)} \middle| x_{1,1}^{(j+1)}, \ldots, x_{N,M}^{(j+1)}\right) = \left\langle x_{1,1}^{(j)}, \ldots, x_{N,M}^{(j)} \right| \exp\left(-\frac{\beta}{J}\hat{H}_M\right) \left| x_{1,1}^{(j+1)}, \ldots, x_{N,M}^{(j+1)} \right\rangle \tag{11}$$

is the high-temperature density matrix of the whole system of M images, and usual boundary conditions are applied: $x_{i,m}^{(J+1)} = x_{i,m}^{(1)}$.

The wavefunctions (*bra*- and *ket*-vectors) in (11) must possess the specified symmetry over particle permutations. They can be built from the wavefunctions of distinguishable particles using symmetrization operation. The same symmetrization operation relates the corresponding density matrices. In the considered case of M images, the symmetrization is made in two steps. First, within each image, symmetrization is made which reflects the physical nature of the particles; that is, if the original particles are fermions, antisymmetric combination of the density matrices for distinguishable particles (see (5), (8)) is used. If the original particles are bosons, the *determinant* in (8) is substituted by a *permutator* [9]. On the second step, antisymmetrization over different images must be made to satisfy the condition that transposition of any two images must change sign of the total wavefunction. Thus the high-temperature density matrix $\Re_M$ of the system of M images is expressed as a determinant,

$$\Re_M^{(j)}\left(x_{1,1}^{(j)}, \ldots, x_{N,M}^{(j)} \middle| x_{1,1}^{(j+1)}, \ldots, x_{N,M}^{(j+1)}\right) = \frac{1}{M!} \times \det \begin{vmatrix} \rho^{(j)}\left(x_{1,1}^{(j)}, \ldots, x_{N,1}^{(j)} \middle| x_{1,1}^{(j+1)}, \ldots, x_{N,1}^{(j+1)}\right) & \ldots & \rho^{(j)}\left(x_{1,1}^{(j)}, \ldots, x_{N,1}^{(j)} \middle| x_{1,M}^{(j+1)}, \ldots, x_{N,M}^{(j+1)}\right) \\ \ldots & \ldots & \ldots \\ \rho^{(j)}\left(x_{1,M}^{(j)}, \ldots, x_{N,M}^{(j)} \middle| x_{1,1}^{(j+1)}, \ldots, x_{N,1}^{(j+1)}\right) & \ldots & \rho^{(j)}\left(x_{1,M}^{(j)}, \ldots, x_{N,M}^{(j)} \middle| x_{1,M}^{(j+1)}, \ldots, x_{N,M}^{(j+1)}\right) \end{vmatrix} \tag{12}$$

with index 'm' (the second subscript) changing from 1 to M along the columns in the left side of ρ and along the rows in the right part of ρ. Elements of this determinant are high-temperature density matrices (short-time propagators) of the original system of N interacting particles. If these are identical fermionic particles, these density matrices coincide with ρ_A in equation (8). In other cases, density matrices for the proper permutation symmetry are used according to [9].

In the case when the original system consists of a single particle, each of the density matrices in the *determinant* on the right-hand side of equation (12) represents a single-particle propagator (equation (3) at $N = 1$) and the approach becomes identical to that of Takahashi for fermions (see section 2.3). Note also that the partition function of the system of M images, Z_M, may be expressed in terms of the partition function of the original system (a single image) by the exact relationships presented in [17].

The Metropolis Monte Carlo procedure is organized in the space of coordinates $\{x_{i,m}^{(j)}\}$ with weights calculated according to equations (8)–(12). A change of coordinate $\{x_{i,m}^{(j)}\}$ causes changes of two density matrices $\Re_M^{(j-1)}$ and $\Re_M^{(j)}$ according to (12). The acceptance

Table 1. Results for two non-interacting fermionic particles in the one-dimensional harmonic oscillator obtained within the PS scheme. ⟨Sign⟩ is the average sign, E_{p+} and E_{p-} are average potential energies for positive and negative permutations, E_p is the resulting potential energy of the two-fermion system. Statistical error is shown in parentheses.

β	J	MC steps	E_{p+}	E_{p-}	E_p	⟨Sign⟩
2	64	10^{10}	0.6560 (0.0005)	0.5176 (0.001)	1.088 (0.006)	0.138 (0.002)
3	64	10^{10}	0.5521 (0.0004)	0.5014 (0.0006)	1.026 (0.013)	0.052 (0.002)
4	64	5×10^{10}	0.5185 (0.0002)	0.5004 (0.0004)	1.0035 (0.01)	0.0187 (0.001)
4	128	10^{11}	0.5189 (0.0003)	0.5009 (0.0006)	1.0031 (0.02)	0.0177 (0.001)
5	64	10^{11}	0.5066 (0.0002)	0.4997 (0.0003)	0.992 (0.04)	0.0075 (0.0007)
6	128	2×10^{11}	0.5024 (0.0002)	0.5002 (0.0003)	0.89 (0.2)	0.0027 (0.0006)

probability of an MC step is then defined as $\min\left(1, \left|\Re_{M\ \mathrm{new}}^{(j-1)}\Re_{M\ \mathrm{new}}^{(j)} \big/ \Re_{M\ \mathrm{old}}^{(j-1)}\Re_{M\ \mathrm{old}}^{(j)}\right|\right)$. The weight function is no longer positive (for $M > 1$) even in the one-dimensional space, but for the case considered below the accompanying sign problem turned out to be not very hard.

The potential energy and particle density can be evaluated directly by simple averaging taking into account sign of the configuration [15]. The ratio of 'positive' and 'negative' configurations, obtained in the MC procedure, is proportional to the ratio of 'positive' (denoted as Z_+) and negative (Z_-) parts of the configurational partition function. The average sign is defined as

$$\langle \mathrm{Sign} \rangle = \frac{Z_+ - Z_-}{Z_+ + Z_-} \tag{13}$$

Averages of physical quantities may be evaluated separately for positive and negative configurations. Then resulting average may be computed as

$$\langle A \rangle = \frac{A_+ Z_+ - A_- Z_-}{Z_+ - Z_-} = \frac{1}{2}\left(\frac{1 + \langle \mathrm{Sign} \rangle}{\langle \mathrm{Sign} \rangle} A_+ - \frac{1 - \langle \mathrm{Sign} \rangle}{\langle \mathrm{Sign} \rangle} A_-\right). \tag{14}$$

In this way, average energy and their contributions, as well as particle density, may be evaluated. The kinetic energy may be evaluated by the primitive estimator obtained by differentiation of the partition function by β and using the following expression for the derivation of determinants [9]:

$$\frac{\partial}{\partial \beta} \det \mathbf{A} = \det \mathbf{A} \cdot \mathrm{Tr}\left(\mathbf{A}^{-1} \frac{\partial}{\partial \beta} \mathbf{A}\right) \tag{15}$$

3. Simulation results

3.1. The one-dimensional harmonic oscillator: permutation sampling

PIMC simulations using the PS algorithm have been carried out for two non-interacting fermionic particles in the one-dimensional harmonic oscillator (potential energy $V(x) = x^2/2$). For two particles, there are only two permutations: the identical one, with the plus sign, which corresponds to two separate closed trajectories for each particle, and the 'exchange' one, with the minus sign, which gives one trajectory linking the both particles. Monte Carlo steps included both displacements of beads of trajectories and change of trajectory linkage.

Simulation results obtained by the PS algorithm are complied in table 1. The values of average potential energy from the identical (positive) permutation, E_+, and exchange (negative)

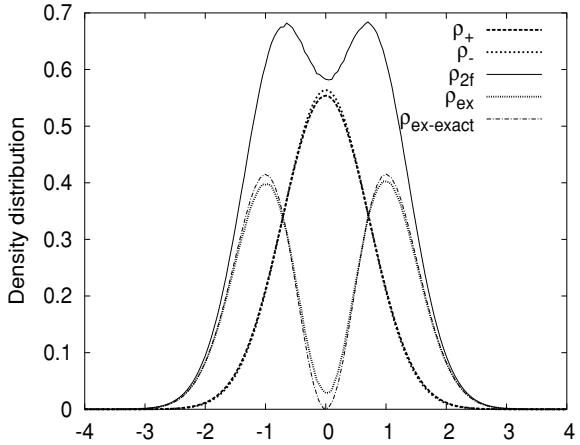

Figure 1. Density distribution for two non-interacting fermions in the one-dimensional harmonic oscillator, for $\beta = 4$ and $J = 64$. ρ_+ and ρ_- are contributions from the positive and negative permutations correspondingly, ρ_{2f} is the resulting density for two fermions, ρ_{ex} is the evaluated density of the first excited state of the harmonic oscillator while $\rho_{\text{ex-exact}} = 2\pi^{-1/2}x^2\,\mathrm{e}^{-x}$ is the exact density of the first excited state.

permutation, E_-, are given. Since, according to the virial theorem, the average kinetic energy of a harmonic oscillator is equal to its potential energy, only values for the computed potential energy are reported. The statistical error here and below was evaluated from the variance of 10 sub-averages calculated during the simulation.

One can see that as the inverse temperature (β) increases, both energies tend to the doubled ground state potential energy of a single particle (0.5), whereas the average sign tends to zero. The potential energy for two fermions, E_p, tends to 1, which is a sum of potential energies of the ground state (0.25) and the first excited state (0.75). For highest β, results become, however, rather uncertain due to the very low value of the average sign.

In figure 1, positive and negative contributions to the coordinate distribution are shown together with the resulting distribution, for $\beta = 4$. Also, a difference between the distributions of two fermions and one fermion is shown, which can be related to the coordinate distribution of the first excited state of the harmonic oscillator. One can see a very good agreement with the exact result $\rho_{\text{ex}} = 2x^2\exp(-x^2)$. In fact, the computed excited state contains an admixture of the second excited state since the temperature is not low enough ($\beta = 4$). One can observe, for example, that the excited state density does not reach zero at zero coordinate as the exact solution does.

The distribution ρ_+ in figure 1 is a little more diffused than distribution ρ_-. When the resulting coordinate distribution ρ is calculated, ρ_+ is multiplied by a slightly larger normalizing factor (see (14)) than ρ_-, and then divided by a small factor $\langle\text{Sign}\rangle$, so that resulting ρ_{2f} becomes positive and normalized by 2. It is important to point out that very accurate evaluation of both ρ_+ and ρ_-, and of the average sign $\langle\text{Sign}\rangle$ are critically important for a reliable evaluation of ρ_{2f} and density of the excited state ρ_{ex}.

For the lowest computed temperature ($\beta = 6$), the average sign becomes about 0.003 with a statistical uncertainty of about 20%. Correspondingly, the statistical error for the energy E_p becomes larger, and further increase of β does not allow us to compute properties of the excited state more precisely than the case $\beta = 4$. For the coordinate distribution, curves similar to that of figure 1 can be drawn for $\beta = 6$, with distributions ρ_+ and ρ_- much closer to

each other and with much more noisy two-fermion density ρ_{2f} and excited state density $\rho_{\rm ex}$ (data not shown).

In fact, at low temperature the resulting two-fermion density is obtained as a tiny difference between contributions of the positive and negative diagrams. The positive diagram corresponds to two distinguishable particles, and its contribution to the particle density is the doubled density of a single particle in the same potential. In the PIMC simulation, this density is generated by two non-interacting ring 'polymers' of length J. The negative diagram corresponds to the trajectory linking the two particles, or to a single closed polymer of length $2J$. This trajectory is also equivalent to the trajectory of a single particle at inverse temperature 2β but with the doubled number of beads [17]. Thus the negative diagram produces coordinate distribution ρ_- which is the doubled coordinate distribution of a single particle at temperature 2β. In fact, in figure 1, the curve for ρ_- perfectly coincides with the doubled ground state coordinate distribution $\rho_0 = \exp(-x^2)/\sqrt{\pi}$, which is not surprising since the effective inverse temperature is $\beta = 8$.

It was shown in [17] that the partition function of N non-interacting fermions can be expressed in terms of partition functions of a single particle at temperatures $\beta, 2\beta, \ldots, N\beta$. Thus the problem of calculation of the $N-1$st excited state may be again recast to the simulation of the original system at temperatures $\beta, 2\beta, \ldots, N\beta$. The problem for numerical calculations is, however, that all properties are expressed as differences of some quantities computed with different β. These differences become exponentially small when $\beta \to \infty$.

Though figure 1 demonstrates a good agreement of the calculated excited state with the exact one, the precision of these calculations cannot be improved significantly even for such a simple model as the one-dimensional harmonic oscillator. Clearly, the systematic error in $\rho_{\rm ex}$ caused by contributions of the higher excited states can be reduced by the increase of β, but this leads to a rapid increase of the statistical error caused by the exponentially small average sign. A simple analysis shows that the problem will be much more severe for a Coulombic potential where the gap between the ground and the first excited state is noticeably larger than between the first and other excited states.

3.2. The one-dimensional harmonic oscillator: an antisymmetric propagator

As was mentioned above, within the AP scheme in one dimension the weight function in (7) is always positive and the sign problem vanishes. Though different ρ_j terms in (7) can be both positive and negative, the total sign is always positive [18]. This is why there is no waste of computer time on the simulation of cancelling contributions. Simulations, carried out for $N = 1, \ldots, 8$ non-interacting fermions in the one-dimensional harmonic oscillator according to expressions (7) and (8), have clearly demonstrated this. The inverse temperature was set to $\beta = 10$ and the number of beads was $J = 200$. Monte Carlo steps were of two kinds. In the first kind of steps (80% of all steps), all N beads corresponding to the same j were displaced by some (different) distances. In the second kind of steps, all the beads belonging to an imaginary time slice from j to $j + l$ were shifted on the same vector. Both kinds of steps require recomputations of two determinants and the corresponding terms of the potential energy. The total number of MC steps in these simulations was 10^{10}.

Since the simulated temperature was very low ($\beta = 10$), the simulated fermions fall into N lowest lying states of the harmonic oscillator, with the contribution of higher states less than $e^{-10} \approx 5 \times 10^{-5}$. Data obtained by the summation of the corresponding states of the harmonic oscillator are therefore considered as 'exact'. Results for the computed potential and kinetic energies are given in table 2 while results for the particle density are displayed in figure 2. The density of the nth excited state can be obtained by subtraction of densities of systems with $n+1$

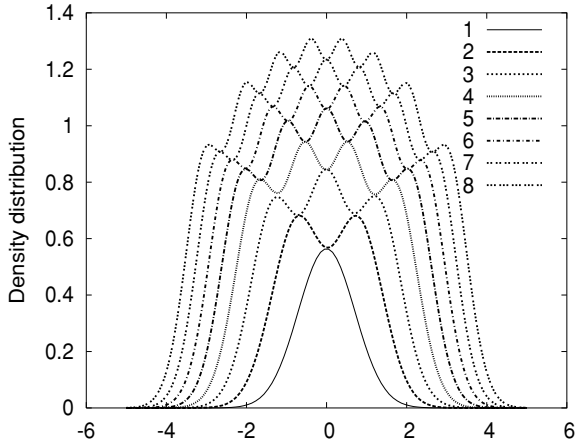

Figure 2. Particle densities of N non-interacting fermions in the one-dimensional harmonic oscillator ($N = 1, \ldots, 8$) calculated by the PIMC method at $\beta = 10$, $J = 200$.

Table 2. The computed potential and kinetic energy of N non-interacting fermionic particles in the one-dimensional harmonic oscillator obtained within the AP scheme. In all the cases, $\beta = 10$ and $J = 200$. 'Exact' potential energy is the sum of potential energies of the N lowest states. Statistical error is shown in parentheses.

N	E_p	E_k	$E_p = E_k$ (exact)
1	0.2497 (0.001)	0.249 (0.002)	0.25
2	0.998 (0.002)	1.001 (0.003)	1.0
3	2.253 (0.005)	2.246 (0.006)	2.25
4	3.995 (0.007)	4.003 (0.007)	4.0
5	6.249 (0.01)	6.246 (0.01)	6.25
6	8.992 (0.01)	8.995 (0.01)	9
7	12.244 (0.01)	12.261 (0.01)	12.25
8	16.001 (0.01)	15.993 (0.01)	16

and n fermions. As an example, coordinate distributions for the second and seventh excited states are given in figure 3 in comparison with exact analytical results ($\rho_{2\mathrm{ex}}(x) = (4x^2 - 2)^2 \exp(-x^2)/(8\sqrt{\pi})$; $\rho_{7\mathrm{ex}}(x) = (128x^7 - 1344x^5 + 3360x^3 - 1680x)^2 \exp(-x^2)/(2^7 7!\sqrt{\pi})$ [19]). One can see absolutely perfect agreement of the simulated results both for the energy and for the particle densities.

Clearly, if one is interested in simulating fermion particles in one dimension, the interactions between the particles can be included without any complications. There may be a number of interesting applications related to the properties of *quantum wires* or *Luttinger liquids* [20]. For interacting particles, one could expect the same level of precision as for the simulation of non-interacting ones. There are no serious limitations on the number of particles or on the temperature. Of course, further increase of β requires increase of the number of beads with the corresponding increase of the simulation time. Also, the increase of the number of particles leads to an increase of the computational time as N^3 (determinant calculations scale as N^3). These computational problems can be dealt with using already known techniques. The key for success in the one-dimensional case is that the sign problem disappears completely, thus simulations of any reasonable number of fermion particles become feasible.

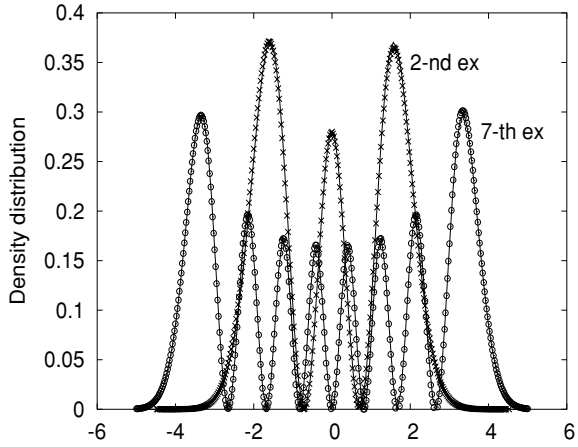

Figure 3. Densities of the second and seventh excited states of the one-dimensional harmonic oscillator (points) calculated by the fermionic PIMC method in comparison with the exact result (lines).

Table 3. Results for non-interacting fermionic particles in the two-dimensional harmonic oscillator ($V(r) = r^2/2$). ⟨Sign⟩ is the average sign, E_{p+} and E_{p-} are average potential energies obtained by positive and negative parts of the weight function correspondingly, E_p is the resulting potential energy. In all the cases, $J = 100$ and the number of MC steps is 2×10^{10}.

N	β	E_p+	E_p-	E_p	⟨Sign⟩
2	6	1.274 (0.001)	1.241 (0.005)	1.507 (0.01)	0.066 (0.001)
2	10	1.255 (0.004)	1.246 (0.02)	1.58 (0.4)	0.0065 (0.002)
3	6	2.217 (0.002)	2.212 (0.02)	2.515 (0.02)	0.0086 (0.0003)
4	6	3.3358 (0.002)	3.3357 (0.002)	3.5 (?)	0.0002 (0.0002)
4	4	3.2582 (0.003)	03.2561 (0.0006)	3.97 (0.1)	0.0016 (0.0003)

3.3. The two-dimensional harmonic oscillator

The arguments showing that the weight function in (7) is positive in one-dimensional case are no longer valid in the case of other dimensions. Some simulation results for several non-interacting fermionic particles in the two-dimensional harmonic oscillator obtained within the AP approach are compiled in table 3.

Let us first examine the results for $N = 2, \beta = 6$. The average sign in this case is not extremely small (above 6%), which allows one to evaluate the total energy with a quite good precision. The temperature is low enough so that this energy can represent the sum of energies of the ground and first excited states which is 1.5. Also, a good agreement is observed between the calculated and exact density distributions (data not shown). Further increase of β leads, however, to the decrease of the average sign and after $\beta = 10$ the results become undetermined.

It is interesting to note that the potential energy, averaged by either positive or negative parts of the wavefunction, E_{p+} and E_{p-}, tends to about 1.25; a value just in the middle of the exact value (1.5) and the value for distinguishable particles (1.0). The last value is also the low-temperature limit for E_{p+} and E_{p-} in the PS scheme (which in this case fails already at $\beta > 3$; data not shown). In some sense, the antisymmetric propagator eliminates about half of the sign problem in this case but another half remains. In other cases considered below (other

Table 4. Results for two non-interacting fermions in the three-dimensional Coulombic potential ($V(r) = -1/r$). ⟨Sign⟩ is the average sign, E_{p+} and E_{p-} are average potential energies obtained by positive and negative parts of the weight function correspondingly, E_p is the resulting potential energy. In all the cases, $J = 500$ and the number of MC steps is 10^{11}.

β	E_{p+}	E_{p-}	E_p	⟨Sign⟩
8	−1.11 (0.1)	−1.74 (0.2)	−0.95 (0.1)	0.66 (0.1)
10	−1.62 (0.05)	−1.82 (0.08)	−1.25 (0.03)	0.27 (0.05)
12	−1.726 (0.02)	−1.83 (0.02)	−1.24 (0.03)	0.10 (0.02)
15	−1.762 (0.01)	−1.795 (0.01)	−1.24 (0.05)	0.04 (0.01)
20	−1.788 (0.007)	−1.793 (0.01)	−1.22 (0.2)	0.005 (0.002)

numbers of particles, the Coulombic potential), E_{p+} and E_{p-} lie between the exact potential energies for fermions and for distinguishable particles, but not necessarily in the middle.

For a larger number of particles, the sign problem becomes more severe even if the antisymmetric propagator is used. For $N = 3$, $\beta = 6$ is in fact the limiting case when accurate enough results can still be obtained (the exact low-temperature limit of E_p is 2.5). For $N = 4$, the average sign at $\beta = 6$ is so low that results become in fact undetermined. Only for $\beta = 4$ a reasonable precision can be reached (the exact low-temperature limit for $N = 4$ is $E_p = 4$).

3.4. The Coulombic potential

The next test was made for two non-interacting fermions in the Coulombic potential in three dimensions. As in the examples above, the dimensionless units are used. Recall that in these units the potential energy of the ground state is -1 and of the first excited state is $-1/4$. Thus in the low-temperature limit for two fermions $E_p = -1.25$. The next excited state has the potential energy $-1/9$. Because of the small energy gap, the first excited energy level is separated from the second only at low enough temperatures.

Note that from the formal point of view, even a single particle in the Coulombic potential is an unstable system at finite temperature: the particle can leave the potential well and go to infinity. To avoid this problem, a hard wall was set on distance $R_{\text{cut}} = 12$ from the centre, which no beads of the trajectories were allowed to cross. Thus a system was put in a finite volume and the problem of a continuum spectrum was removed. In practical simulations, only at the highest considered temperatures ($\beta = 8$ and 10) the trajectories sometimes touched the wall. Another cutoff was set on small distances to the centre to avoid singularity of the Coulombic potential at zero: for distances $r < r_{\text{cut}} = 0.05$, the potential was set to a constant value $V(r) = -1/r_{\text{cut}}$. It was demonstrated elsewhere that even larger cutoffs do not shift noticeably the value of the potential energy [21].

Results for a number of values of β are complied in table 4. It is interesting to note that the result corresponding to the sum of two lowest energy levels, -1.25, is reached already at $\beta = 10$ which may be of surprise since the gap between the first and upper excited states is not large for this value of β. Of course, partial cancelling of different errors may take place, so that contributions from the higher lying states may be compensated by not very large (for the Coulombic potential) number of beads $J = 500$ as well as by the two cutoffs at small and large distances. The calculated density of the first excited state was not in a good agreement with the analytical one (1:3 mixture of 2 s and 1p orbitals; data not shown) because of contributions from the higher energy levels. Further increase of β above 20 is not feasible because the average sign becomes too low (note that a hydrogen atom at 'room' temperature corresponds to $\beta \approx 1000$). The conclusion is that even the AP approach is not able to resolve the sign problem for electrons in atoms at normal temperatures.

Table 5. Potential, kinetic and total energies of two antisymmetric images of N non-interacting fermionic particles in the one-dimensional harmonic potential. The lower part of the table shows the energies of the first excited state of N particles obtained by subtraction of the ground state energy given in table 2. Statistical error is shown in parentheses.

Two antisymmetric images					
N	β	E_p	E_k	$E_{\rm tot}$	⟨Sign⟩
2	10	2.488 (0.005)	2.509 (0.01)	4.997 (0.01)	0.05 (0.001)
3	10	5.016 (0.01)	4.996 (0.02)	10.012 (0.02)	0.011 (0.0005)
4	8	8.485 (0.02)	8.511 (0.02)	16.996 (0.03)	0.007 (0.0005)
5	8	13.05 (0.05)	12.99 (0.05)	26.04 (0.07)	0.003 (0.0003)

First excited state				
N	E_p	E_k	$E_{\rm tot}$	$E_{\rm tot}$ exact
2	1.49	1.5	2.99 (0.01)	3.0
3	2.763	2.751	5.514 (0.02)	5.5
4	4.49	4.502	8.99 (0.03)	9.0
5	6.79	6.74	13.54 (0.07)	13.5

3.5. Excited states of several electrons in one-dimensional harmonic confinement

Finally, an attempt was made to compute the first excited state for several particles. From 2 to 5 fermionic particles ($N = 2 - 5$), interacting by the Coulombic potential $V(r) = e^2/r$, were placed in the harmonic potential well $V_{\rm ex} = r^2/2$ in one dimension. The ground state of this system was simulated according to section 2.3 at low temperature. To compute the first excited state, two images of the original system with permutation antisymmetry between them were considered according to section 2.4.

The case of non-interacting particles ($e = 0$) was also considered in order to check that the method of excited state calculations for several particles according to equations of section 2.4 works properly. The expected result is that in the first excited state of N non-interacting fermions, $N - 1$ fermions occupy the $N - 1$ lowest states while the Nth fermion occupies the $(N + 1)$th state. The computed results for the energy, presented in table 5, show perfect agreement with the analytical results. Also, excellent agreement was found for the density distributions (data not shown).

Note, however, that the total weight function in (10) for two antisymmetric images of a system of $N \geqslant 2$ particles is no longer positive even in one dimension. Practical simulations in the one-dimensional harmonic oscillator have shown, however, that the sign problem is not too hard in this case and allows us to obtain accurate enough results even at $\beta = 10$ which provides a reliable separation of the ground and excited states. For cases N = 4 and 5 the inverse temperature $\beta = 8$ was used. Though the average sign in these cases was rather low, its relative fluctuations during the simulations were also small, which allowed us to reach a good precision.

Results for different contributions to energy for charged fermions in the one-dimensional harmonic oscillator are presented in table 6. The number of MC steps in double-image simulations was 5×10^{10} while in the standard simulations of N interacting particles the number of steps was 10^{10}. Note that since in the last case the sign was always positive, even a smaller number of MC steps provided a higher accuracy. One can see, for example, that while the energy gap between the ground and the first excited state remains about 1 for two fermions with different charges, it decreases to about 0.8 for four or five charged fermions. As another example, the distribution densities of five electrons ($e = 1$) in the ground and the

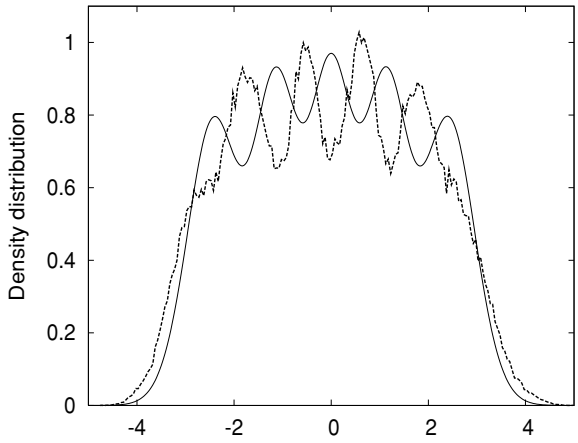

Figure 4. Densities of the ground (the solid line) and the first excited (the dashed line) states of five polarized electrons in the external harmonic field in one dimension.

Table 6. Contributions to energy: potential external (E_h), interaction (E_e), kinetic (E_k) and total energies of N charged fermionic particles in the one-dimensional harmonic potential. Upper part: the result for two antisymmetric images of the system. Middle part: a single image (in fact, the standard simulation of N interacting electrons). Lower part: energies of the first excited state of N charged fermionic particles. $\beta = 10$ for $N = 2, 3$ and $\beta = 8$ for $N = 4, 5$.

N	e	E_h	E_e	E_k	E_{tot}	⟨Sign⟩
			Two antisymmetric images			
2	1	2.894	1.338	2.233	6.455 (0.003)	0.0417 (0.0004)
2	2	3.937	3.907	1.992	9.836 (0.004)	0.0329 (0.0004)
2	3	5.322	6.831	1.929	14.083 (0.007)	0.0309 (0.0003)
2	4	6.926	10.056	1.898	18.881 (0.01)	0.0299 (0.0002)
3	1	6.155	3.847	4.124	14.126 (0.01)	0.0063 (0.0003)
4	1	10.63	7.53	6.74	24.90 (0.02)	0.0044 (0.0002)
5	1	16.48	12.16	10.25	38.89 (0.04)	0.0028 (0.0002)
			Single image (ground state)			
2	1	1.189	0.671	0.859	2.721 (0.001)	1
2	2	1.720	1.954	0.741	4.414 (0.001)	1
2	3	2.421	3.410	0.712	6.542 (0.001)	1
2	4	3.217	5.023	0.701	8.941 (0.001)	1
3	1	2.817	1.933	1.840	6.590 (0.002)	1
4	1	5.086	3.753	3.208	12.047 (0.002)	1
5	1	8.026	6.080	4.950	19.046 (0.002)	1
			First excited state			
2	1	1.697	0.671	1.359	3.726 (0.003)	
2	2	2.217	1.953	1.251	5.421 (0.004)	
2	3	2.902	3.421	1.217	7.540 (0.007)	
2	4	3.709	5.033	1.197	9.94 (0.01)	
3	1	3.338	1.914	2.284	7.536 (0.01)	
4	1	5.54	3.78	3.53	12.85 (0.02)	
5	1	8.46	6.08	5.30	19.84 (0.04)	

first excited states are shown in figure 4. One can see how the distances between the maxima of the density distribution increase comparing to the uncharged case in figure 2.

4. Conclusion

This paper introduces a novel method of the path integral Monte Carlo simulation of excited states of a single or of several interacting quantum particles in an external field. A number of images of the original system are introduced with the requirement of the antisymmetry of the total wavefunction over permutations of the images. As a result, at low temperature the images occupy the lowest eigenstates of the system according to the build-up principle.

For the case of a single particle in an external field, the problem of computation of excited states is equivalent to the problem of several non-interacting fermions in the same field. Several exactly solvable models were considered: one- and two-dimensional harmonic oscillators and the Coulombic potential. The energies and coordinate distributions of excited states were computed and compared with the exact results with the purpose of defining limits of applicability of the developed approach. Since PIMC simulations of a system with an antisymmetric wavefunction result in the sign problem, such simulations become feasible only in the cases when the sign problem can be resolved in a reasonable way. It was shown that as long as the average sign of the weight function is not vanishingly small (above $\approx 10^{-3}$), the method allows us to compute properties of excited states with an acceptable precision.

The average sign is, however, not an intrinsic characteristic of the considered system, but it is strongly affected by the choice of the simulation scheme. The example of non-interacting fermionic particles in the one-dimensional harmonic oscillator shows that the choice of the method to treat the antisymmetry of the wavefunction may have a very strong impact on the average sign and on the possibilities of extracting properties of excited states from PIMC simulations. In the case of the PS scheme, it was only possible to evaluate the density of the first excited state of the one-dimensional harmonic oscillator with a few per cent precision. However, in the case of the AP scheme applied to the same system, very accurate estimations of the densities of up to at least the eighth excited state become possible. The key to success lies in the fact that the AP scheme solves the sign problem completely, providing a strictly positive weight function for fermions in one dimension.

For systems of higher dimensions, the AP scheme only relaxes the sign problem relative to the PS approach. The expression for the weight of configurations, presented as determinants in (8), makes the beads at imaginary times j and $j+1$ gather in pairs, when each bead at time j attracts effectively a single bead at time $j+1$ (belonging to any particle), while different pairs of such beads repel each other and a system of linked 'threads' is formed. In each thread, the order of particles is random, since permutations of any particles do not change the weight function in (7). The overall picture resembles the trajectories in the PS approach, with the total negative sign if the structure of linked threads corresponds to the negative diagram. The difference is, however, that in the case of an antisymmetric propagator, the threads effectively repel each other. Thus, in the low-temperature limit, the system does not fall into the ground state of distinguishable particles, but adopts a more extensive configuration, with higher energy than the corresponding system of distinguishable particles. For a particle in the two-dimensional harmonic oscillator, it turned out to be possible to compute several lowest lying excited states if the AP scheme is used. For a particle in a three-dimensional Coulombic field, the sign problem does not allow a reasonable computation even of the first excited state.

The method introduced can also be used for the simulation of excited states of a system of interacting particles. This is the most interesting case since there are no analytical or numerical approaches which are able to treat exactly the correlation and exchange effects for several interacting particles. However, the sign problem appears here even if the interacting particles are in one dimension. Still, computation of the first excited state turned out to be

possible for several particles interacting by a repulsive Coulombic potential in a harmonic well.

This paper also demonstrates the interconnection between the sign problem and simulations of excited states within the PIMC method. It is clear that the solution of the excited states problem relies completely on the solution of the sign problem. On the other hand, computation of excited states may be a very sensitive test of different (and especially approximative) approaches to deal with the sign problem.

Acknowledgment

The work has been supported by the Swedish Research Council (Vetenskapsrådet).

References

[1] Barker J A 1979 *J. Chem. Phys.* **70** 2914
[2] Ceperley D M 1992 *Phys. Rev. Lett.* **69** 331
[3] Mak C H, Egger R and Weber-Gottschick H 1998 *Phys. Rev. Lett.* **81** 4533
[4] Egger R, Mühlbacker L and Mak C H 2000 *Phys. Rev.* E **61** 5961
[5] Zhang S, Carlson J and Gubernatis J E 1997 *Phys. Rev.* B **55** 7464
[6] Helenius P and Sandvik A W 2000 *Phys. Rev.* B **62** 1102
[7] Dikovsky M V and Mak C H 2001 *Phys. Rev.* B **63** 235105
[8] Pollock E L and Ceperley D M 1984 *Phys. Rev.* B **30** 2555
[9] Takahashi M and Imada M 1984 *J. Phys. Soc. Japan* **53** 963
[10] Feynman R P and Hibbs A R 1965 *Quantum Mechanics and Path Integrals* (New York: McGraw-Hill)
[11] Lyubartsev A P and Vorontsov-Velyaminov P N 1993 *Phys. Rev.* A **48** 4075
[12] Høye J S and Steel G 1994 *J. Stat. Phys.* **77** 361
[13] Shevkunov S V 2000 *J. Exp. Theor. Phys.* **118** 31
[14] Miura S and Okazaki S 2000 *J. Chem. Phys.* **112** 10116
[15] Loh E Y *et al* 1990 *Phys. Rev.* B **41** 9301
[16] Nakamura T 1998 *Phys. Rev.* B **57** R3197
[17] Vorontsov-Velyaminov P N, Ivanov S D and Gorbunov R I 1999 *Phys. Rev.* E **59** 168
[18] Ceperley D M 1996 *Path Integral Monte Carlo Methods for Fermions* ed K Binder and G Cicotti (Bologna: Editrice Compositori) simulation in condensed matter, physics and chemistry edition
[19] Atkins P W 1999 *Physical Chemistry* (Oxford: Oxford University Press)
[20] Wang D W, Millis A J and Sarma S D 2004 *Solid State Commun.* **131** 637
[21] Ivanov S D, Lyubartsev A P and Laaksonen A 2003 *Phys. Rev.* E **67** 066710